JCTC Journal of Chemical Theory and Computation

pubs.acs.org/JCTC Article

Subspace-Search Quantum Imaginary Time Evolution for Excited State Computations

Cameron Cianci,* Lea F. Santos, and Victor S. Batista

Cite This: https://doi.org/10.1021/acs.jctc.4c00915 Read Online

ACCESS | Metrics & More | Article Recommendations

ABSTRACT: Quantum systems in excited states are attracting significant interest with the advent of noisy intermediate-scale quantum (NISQ) devices. While ground states of small molecular systems are typically explored using hybrid variational algorithms like the variational quantum eigensolver (VQE), the study of excited states has received much less attention, partly due to the absence of efficient algorithms. In this work, we introduce the *subspace search quantum imaginary time evolution* (SSQITE) method, which calculates excited states using quantum devices by integrating key elements of the subspace search variational quantum eigensolver (SSVQE) and the variational quantum imaginary time evolution (VarQITE) method. The effectiveness of SSQITE is demonstrated through calculations of low-lying excited states of benchmark model systems including H_2 and LiH molecules. A toy Hamiltonian is also employed to demonstrate that the robustness of VarQITE in avoiding local minima extends to its use in excited state algorithms. With this robustness in avoiding local minima, SSQITE shows promise for advancing quantum computations of excited states across a wide range of applications.

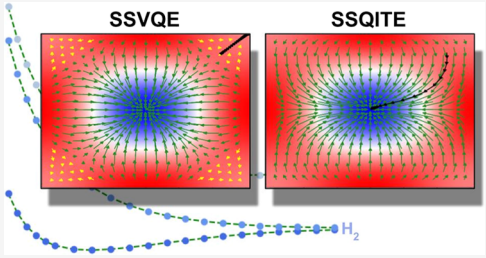

1. INTRODUCTION

Computational and theoretical studies of excited states are essential for understanding the photophysics of molecules, particularly in ultraviolet−visible (UV−vis) and X-ray absorption spectroscopy of photochemical reactions.[1,2] With the advent of quantum computing, new methodologies promise to significantly enhance these studies, potentially offering a quantum advantage in chemistry.[3,4] Traditional computational methods, despite their powerful capabilities, face limitations in modeling complex excited state phenomena due to the exponential scaling of resources required. Quantum computing, however, opens new frontiers for exploring a wide range of problems,[5,6] including the crucial excited states in the photochemistry of organic molecules.[7]

In the near-term intermediate-scale quantum (NISQ) era, quantum advantage of some specialized applications have already been put forward,[8,9] such as the calculation of ground state energy in quantum chemistry.[10−12] Widespread approaches for calculating ground state energies in quantum computers include the hybrid variational quantum eigensolver (VQE) algorithm[10,12,13] or the variational quantum imaginary time evolution (VarQITE) method.[13−15] Beyond ground state energies, excited states are equally important for numerous applications,[16−21] such as charge and energy transfer in photovoltaic materials, photodissociation,[22] luminescence,[7] intermediate states in chemical reactions,[23] and mechanistic studies of catalytic systems.[24] This has driven significant interest in generalizing ground state algorithms, such as VQE and VarQITE, to excited states of quantum systems. Notable algorithms designed for this purpose include the subspace-search variational quantum eigensolver (SSVQE)[25] and the variational quantum deflation (VQD)[22] algorithm. The VQD approach[22] has been applied to calculations at Frank−Condon and the conical intersection geometries,[26] and has been adapted to VarQITE[27,28] for determining excited states.

Quantum algorithms for the imaginary time evolution have proven useful in the determination of both ground and excited states. There are two quantum algorithms that can perform imaginary time evolution in quantum computers, variational quantum imaginary time evolution (VarQITE),[13,29,30] and trotterized quantum imaginary time evolution (TrotterQITE).[31] VarQITE uses a variational circuit to approximate the evolution of the input state through imaginary time, whereas TrotterQITE implements a nonunitary imaginary time step $e^{-\mathcal{H}d\tau}$ by applying a normalized unitary time step $e^{-iAd\tau}$ with ancilla qubits. Due to the ancilla qubits, TrotterQITE requires many more qubits and a larger gate depth than VarQITE. Due to the fixed gate depth and therefore greater noise resilience of VarQITE, this algorithm is used in the excited state algorithm presented.

Received: July 15, 2024
Revised: September 16, 2024
Accepted: September 18, 2024

Imaginary time algorithms have been applied to determine excited states through other methods, such as subspace expansion methods.[32] Subspace expansion methods define a subspace of the system using nonorthogonal states, with the exception of multistate contracted VQE,[33] and classically diagonalize this subspace using the generalized eigenvalue equation,[33−36] rather than minimizing the entire Lagrangian as is performed in VQE or VarQITE. These subspace expansion methods perform well when the input states have a large overlap with the low-energy states of interest. For this reason, TrotterQITE has been used in conjunction with subspace expansion, referred to as Krylov subspace methods.[31,32,37,38] These algorithms have accuracy guarantees but can require deep quantum circuits to perform TrotterQITE. Comparing subspace expansion to subspace search, the subspace expansion does not yield an orthonormal set of states, whereas subspace search ensures orthogonality of the output states.

In this article, we introduce a novel algorithm called subspace search quantum imaginary time evolution (SSQITE). The SSQITE algorithm augments VarQITE with a subspace search to compute excited states to enable the simultaneous calculation of ground and multiple excited states. Its efficiency is successfully demonstrated with the calculation of the low-lying states of H_2 and LiH molecules. The paper is organized as follows. First, we introduce the SSVQE and VarQITE methods in Sections 2 and 3, respectively. Then, we describe the SSQITE algorithm in Section 4 and illustrate its application to calculations of excited states of H_2 and LiH, as well as introduce a toy Hamiltonian to demonstrate SSQITE's robustness to local minima in Section 5. Conclusions are presented in Section 6.

2. SUBSPACE-SEARCH VARIATIONAL QUANTUM EIGENSOLVER

The subspace-search variational quantum eigensolver (SSVQE) algorithm extends the variational quantum eigensolver (VQE) hybrid method.[10,12] The VQE is a hybrid quantum-classical algorithm designed to find the ground state of a quantum system described by the $2^n \times 2^n$ Hamiltonian, H, expressed as a sum of tensor products of Pauli matrices $\sigma_k^{(j)} = \{X, Y, Z, I\}$,

$$H = \sum_j c_j \bigotimes_{k=1}^{n} \sigma_k^{(j)} \tag{1}$$

where $c_j = 2^{-n}\mathrm{Tr}[H \times \otimes_{k=1}^{n} \sigma_k^{(j)}]$. VQE generates a trial state $|\psi(\vec{\theta})\rangle = U(\vec{\theta})\,|\psi_0\rangle$ by applying a quantum circuit $U(\vec{\theta})$ with variational parameters $\vec{\theta}$ to an initial vacuum state $|\psi_0\rangle$. These parameters are adjusted by a classical computer to minimize the expectation value of the Hamiltonian, $E(\vec{\theta}) = \langle\psi(\vec{\theta})|\hat{H}|\psi(\vec{\theta})\rangle$. This expectation value is computed by summing the expectation values of the tensor products of Pauli matrices, $\langle\psi(\vec{\theta})| \otimes_{k=1}^{n} \sigma_k^{(j)}|\psi(\vec{\theta})\rangle$, measured on the quantum computer. The process iteratively refines $\vec{\theta}$ to minimize $E(\vec{\theta})$, thereby approximating the lowest eigenvalue of H.

SSVQE extends the VQE algorithm to simultaneously find the k lowest eigenstates of H.[25] First, the k orthogonal states $|\phi_j\rangle$ are initialized with $\langle\phi_k|\phi_j\rangle = \delta_{kj}$. These states are then evolved using the same circuit $U(\vec{\theta})$ with variational parameters $\vec{\theta}$. Orthogonality is thus preserved among the evolved states since $U(\vec{\theta})^\dagger U(\vec{\theta}) = I$, so $\langle\phi_k|U(\vec{\theta})^\dagger U(\vec{\theta})|\phi_j\rangle = \delta_{kj}$. The ansatz defining the circuit $U(\theta)$ can be chosen to preserve the symmetry, such as the "ASWAP" ansatz which is constructed using gates that preserve the number of excitations in a state.[39]

The parameters $\vec{\theta}$ are optimized by minimizing the sum of the expectation values using the following loss function

$$\mathcal{L}_\omega(\vec{\theta}) = \sum_{j=0}^{k} \omega_j \langle\phi_j|U^\dagger(\vec{\theta})\mathrm{H}U(\vec{\theta})|\phi_j\rangle \tag{2}$$

Therefore, SSVQE finds the k orthogonal minimum energy states simultaneously. The coefficients ω_i, introduced by eq 2, with $\omega_i > \omega_j$ for $i < j$, are used to weight each energy level, effectively arranging the energy expectation values of all orthogonal states in ascending order.

In this paper, we introduce the subspace search quantum imaginary time evolution (SSQITE) algorithm by integrating this SSVQE methodology of orthogonal states with the VarQITE algorithm.[13,14] The resulting SSQITE method thus enables the simultaneous calculation of multiple excited states by applying the same imaginary time evolution to an initial set of orthogonal states.

3. VARIATIONAL QUANTUM IMAGINARY TIME EVOLUTION

The variational quantum imaginary time evolution (VarQITE) algorithm is a hybrid quantum-classical method used to determine the ground state energy of a quantum system by propagating an initial state $|\psi(0)\rangle$ in imaginary time toward $|\psi(\tau)\rangle$, where $\tau = it/\hbar$ is the imaginary time.[13,14] This technique effectively implements the Wick-rotated Schrödinger equation,

$$\frac{\mathrm{d}}{\mathrm{d}\tau}|\psi(\tau)\rangle = -(\mathcal{H} - E_\tau)|\psi(\tau)\rangle \tag{3}$$

with $E_\tau = \langle\psi(\tau)|\mathcal{H}|\psi(\tau)\rangle$. Propagating that initial state for a sufficiently long imaginary time, we obtain the ground state $|E_0\rangle$, provided that $\langle E_0|\psi(0)\rangle \neq 0$. This is expressed as follows

$$\lim_{\tau\to\infty} A(\tau)\mathrm{e}^{-H\tau}|\psi(0)\rangle = |E_0\rangle \tag{4}$$

where $A(\tau) = \langle\psi(0)|e^{-2H\tau}|\psi(0)\rangle^{-1/2}$ is the normalization factor obtained after imaginary time propagation. To apply this procedure to a given parametrized ansatz $|\psi(\tau)\rangle = U(\theta(\tau))\,|0\rangle$, McLachlan's variational principle can be leveraged, which states

$$\delta\left|\left|\left(\frac{d}{d\tau} + \mathcal{H} - E_\tau\right)|\psi(\tau)\rangle\right|\right| = 0 \tag{5}$$

Applying this principle to the optimization of the variational parameters $\vec{\theta}$ that define $U(\vec{\theta}(\tau))$ results in the following linear system of ordinary differential equations:[13,14]

$$\sum_j A_{ij}\dot{\theta}_j = C_i \tag{6}$$

where

$$A_{ij} = \Re\left(\frac{\partial\langle\phi(\vec{\theta}(\tau))|}{\partial\theta_i}\frac{\partial|\phi(\vec{\theta}(\tau))\rangle}{\partial\theta_j}\right) \tag{7}$$

and

https://doi.org/10.1021/acs.jctc.4c00915
J. Chem. Theory Comput. XXXX, XXX, XXX−XXX

$$C_i = -\Re\left(\langle \frac{\partial\phi(\vec{\theta}(\tau))}{\partial\theta_i} \middle| \mathcal{H}|\phi(\vec{\theta}(\tau))\rangle\right) \tag{8}$$

The values of A_{ij} and C_i are obtained using the Hadamard test on a quantum circuit by simply averaging the measurements on the ancilla qubit.[13]

Having obtained A_{ij} and C_i by measurements of the ancilla in the quantum circuit, the values of $\vec{\theta}$ are updated in a classical computer by integrating the Euler equation introduced by eq 6 using the fourth-order Runge−Kutta method.[40] The process is iterated until the values of $\vec{\theta}$ converge to optimum values, as determined by McLachlan's variational principle introduced by eq 5.

4. SUBSPACE-SEARCH QUANTUM IMAGINARY TIME EVOLUTION

The subspace-search quantum imaginary time evolution (SSQITE) method, proposed in this paper, combines subspace search optimization with variational quantum imaginary time evolution to maintain orthogonality among states evolving in imaginary time. This approach allows for the simultaneous variational computation of both ground and excited energy states by using variational quantum imaginary time evolution.

The main difficulty in combining the subspace search optimization with variational quantum imaginary time evolution is that the imaginary time propagation only implicitly optimizes the loss function defined by McLachlan's variational principle in eq 5. Instead of defining a joint loss function, as in SSVQE, the SSQITE algorithm tunes the step size $d\tau_j$ of each level j individually, such that lower energy states have larger integration time steps (pseudocore, Algorithm 1). Intuitively, this allows for lower energy states to overpower the higher energy states, ordering the output energy spectrum. The tuning of time steps plays a role similar to that of the tuning of the weights ω_i in the SSVQE algorithm. In this way, after a sufficient number of iterations, the SSQITE algorithm returns the k-lowest-energy eigenstates.

The choice of weights ω_i can greatly impact the convergence of the algorithm, and has been previously chosen to take advantage of the choice of input states and ansatz, system size, or symmetries.[19,41] For example, the weight selection for the fastest convergence of CQE on H_2 was found to be $\omega_i = [9, 9, 1, 1]$,[19] as it takes advantage of the block-diagonal nature of the Hamiltonian. Here, we will instead demonstrate a weight setting scheme that utilizes the nature of orthogonal states evolving under VarQITE to prevent the evolution of higher energy states from overpowering lower energy states while retaining an efficient runtime.

In this weight setting scheme, the integration time steps are defined as follows

$$d\tau_i = \frac{b}{2^i} \tag{9}$$

with b a tunable parameter. This choice of integration time steps prevents higher energy levels from overpowering lower energy eigenstates, since

$$\frac{1}{2^i} \geq \sum_{j=i+1}^{k} \frac{1}{2^j} \tag{10}$$

However, this approach requires a number of steps that scales exponentially as $O(2^k)$, where k is the size of the subspace. This exponential scaling can be overcome by leveraging the convergence of the lower energy levels. The integration time steps used for obtaining higher energy levels can be increased upon convergence of lower energy states since all remaining states must be orthogonal to the manifold of lower energy states $\langle E_j|\psi_i\rangle \approx \delta_{ji}$ for $i > j$. Therefore, the imaginary time evolution of higher excited states is restricted to an orthogonal subspace.

Due to the time evolution of excited states being restricted, the integration time step of these states can be doubled, mitigating the exponential scaling without significantly affecting the lower energy states. However, the imaginary time evolution of the ground state makes the overlap with excited states exponentially small, although not exactly zero, $\langle E_0|\psi_i\rangle \approx e^{-\tau}$. Therefore, in practice, some excited states can still evolve into the ground state if they are not fully orthogonalized. So, it is always necessary to confirm orthogonality with lower energy states during each round of SSQITE.

Algorithm 1 Pseudo-code for the SSQITE Algorithm

```
Require: ψ = ψ_i, with 0 ≤ i < k.
Ensure: ⟨ψ_i|ψ_j⟩ = δ_ij
  while not all_converged(θ̇) do
      dτ_i ← {1/2^i | 0 ≤ i < k}                          ▷ Initialize Step Sizes
      A_ijl ← Measure_A(U(θ⃗)ψ_l)
      C_il ← Measure_C(U(θ⃗)ψ_l)
      θ̇_jl ← A^{-1}_ijl C_il                              ▷ Calculate θ̇
      for l = 0, l < k, l++ do
          if converged(θ̇_l) then
              for i = l, i < k, i++ do
                  dτ_i ← 2 * dτ_i                         ▷ Avoid Exponential Scaling with k
              end for
          end if
      end for
      for j = 0, j < num_params, j++ do
          for l = 0, l < k, l++ do
              θ_jl ← θ_jl + dτ_l * θ̇_jl                   ▷ Update Theta
          end for
      end for
  end while
```

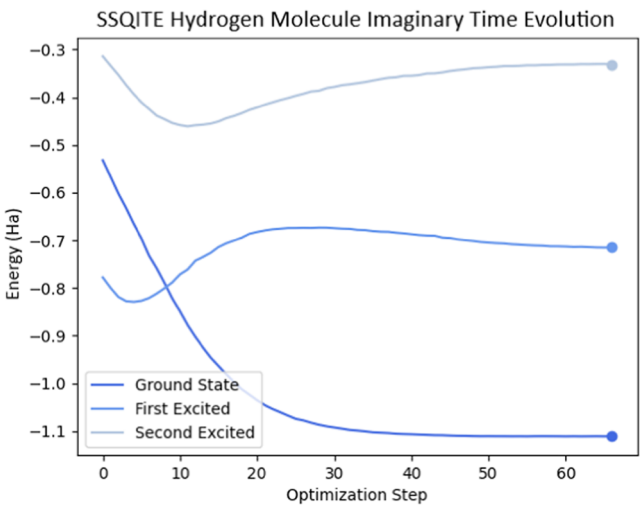

Figure 1. Simultaneous evolution of the energy expectation values for the three lower energy states of H_2 (with fixed bond length R = 0.95 Å) during the first 70 integration steps of SSQITE optimization. Final energy values are highlighted on the right, and corresponding statistical errors are on the order of 10^{-5} Ha.

https://doi.org/10.1021/acs.jctc.4c00915
J. Chem. Theory Comput. XXXX, XXX, XXX−XXX

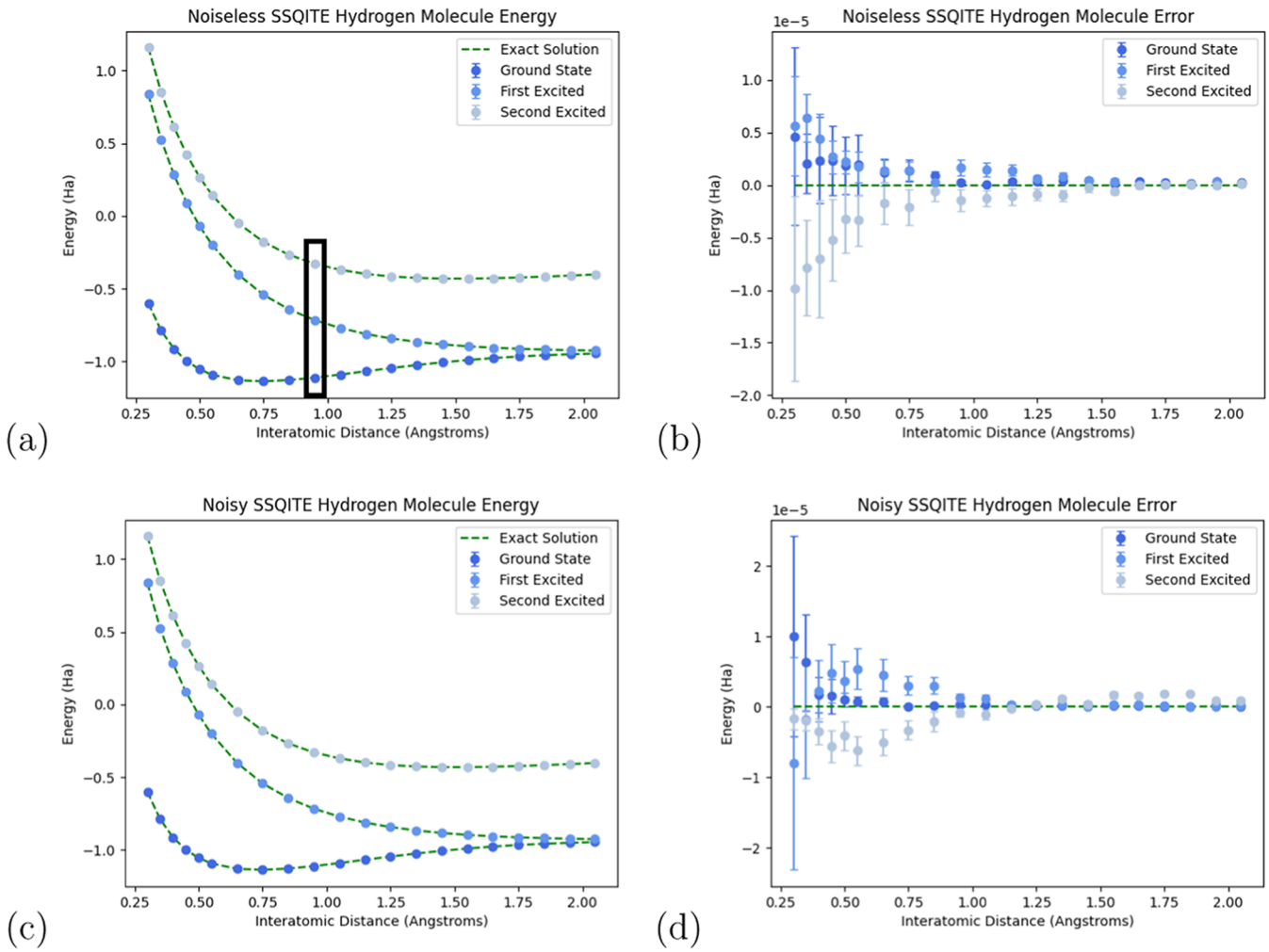

Figure 2. Comparison of the three lowest energy eigenvalues of H_2 determined through (a, b) noiseless and (c, d) noisy SSQITE optimization to numerically exact calculations (dashed lines) as a function of the interatomic HH distance. Boxed values correspond to the final values shown in Figure 1. The ground, first, and second excited states correspond to the $X^1\Sigma_g^+$, $b^3\Sigma_u^+$, and $B^1\Sigma_u^+$ states of H_2, respectively. Deviations of (b) noiseless and (d) noisy SSQITE calculations from the ground truth energy levels of the H_2 molecule. All noisy simulations are performed by using the qiskit FakeSherbrooke backend.

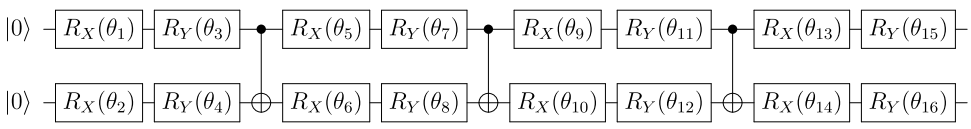

Figure 3. Variational quantum circuit ansatz with two qubits used for the SSQITE H_2 calculations shown in Figure 2. The TwoLocal ansatz involves one layer of parametrized RX and RY gates, followed by a CNOT gate. This ansatz is general, in the sense that it can realize any two-qubit operation.

5. RESULTS: GROUND AND EXCITED STATES OF H_2 AND LIH

SSQITE was implemented on H_2 by using a two-qubit Hamiltonian. This H_2 Hamiltonian was created by beginning with the STO-3G basis and selecting for the spin-zero subspace to provide four states, which can be directly mapped to two-qubit states.[35] This Hamiltonian has previously been used in conjunction with quantum subspace expansion, achieving an error far exceeding chemical accuracy for a range of interatomic distances.[35]

Figure 1 illustrates the energy expectation values for the three lowest energy states of H_2 during joint SSQITE optimization (with a fixed H−H bond length of 0.95 Å). The imaginary time propagation causes these states to interfere with their contributions to $\vec{\theta}$. As shown in Figure 1, the evolution of the ground state for $\tau \in [0, 20]$ leads to an increase in the energy of the first excited state, as it is forced into a subspace orthogonal to the ground state. This effect is also reciprocal, since the evolution of the first excited state likely slows the evolution of the ground state, as evidenced by the linear slope of the ground state from $\tau = 0$ to $\tau = 15$.

Figure 2(a,c) shows the three lowest energy eigenvalues of H_2 determined through SSQITE optimization. These calculations use a general two-qubit ansatz depicted in Figure 3, as a function of the interatomic H−H distance.[35] These results demonstrate excellent agreement with exact results for both noiseless (Figure 2(a)) and noisy (Figure 2(c)) quantum

https://doi.org/10.1021/acs.jctc.4c00915
J. Chem. Theory Comput. XXXX, XXX, XXX−XXX

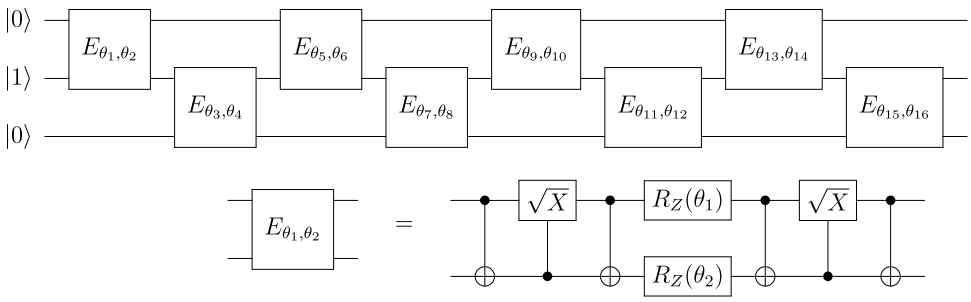

Figure 4. Top: Variational quantum circuit ansatz with three qubits used for the SSQITE LiH calculations shown in Figure 5 is based on a custom excitation preserving ansatz. Bottom: Excitation preserving subcircuit with two tunable parameters.

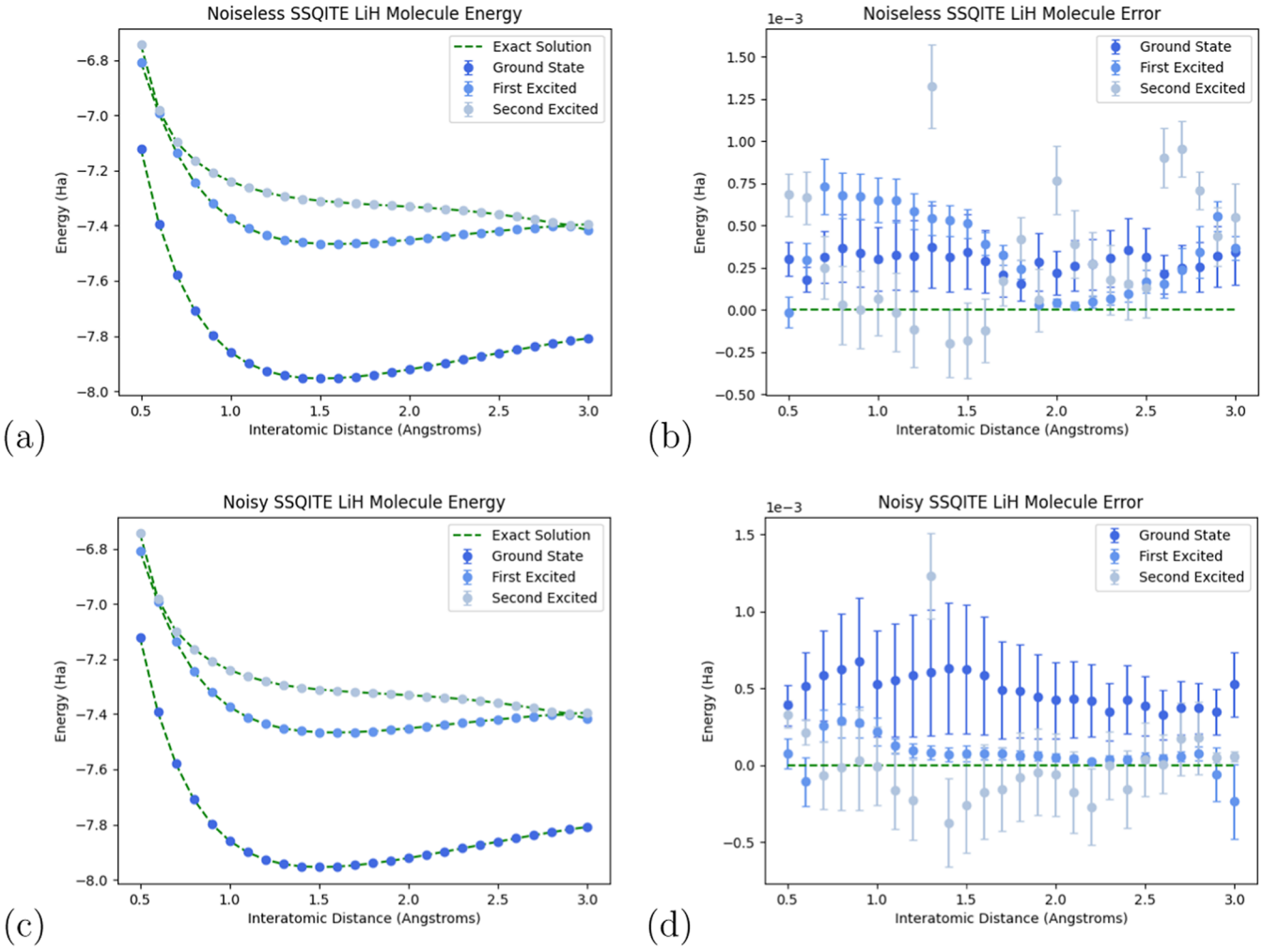

Figure 5. Comparison of the three lowest energy eigenvalues of LiH determined through (a, b) noiseless and (c, d) noisy simulation of SSQITE optimization to numerically exact calculations (dashed lines). The ground, first, and second excited states correspond to $X^1\Sigma^+$, $a^3\Sigma^+$, and $A^1\Sigma^+$, respectively. Note that the results from LiH differ from experimental data due to the truncated atomic orbital basis set used. Depicted are the deviations of the (b) noiseless and (d) noisy SSQITE calculations from the ground truth energy levels of the LiH molecule. All noisy simulations are performed using the qiskit FakeSherbrooke backend.

simulators. In fact, the comparison to numerically exact calculations shown in Figure 2(a,c) demonstrates the accuracy and capabilities of the SSQITE algorithm over the entire range of bond lengths.

Figure 2(b) [Figure 2(d)] shows the errors of the noiseless [noisy] SSQITE calculations for the H_2 molecule, which remain within 9.8×10^{-6} Ha (1.0×10^{-5} Ha), i.e., within chemical accuracy of 1.6×10^{-3} Ha.[22]

For comparison, we also apply the SSQITE algorithm to the LiH molecule,[42] using a custom excitation preserving ansatz with 16 adjustable parameters shown in Figure 4. This excitation preserving ansatz ensures that the occupation number symmetry is preserved by SSQITE. The three-qubit LiH Hamiltonian is obtained by beginning with the STO-6G basis. Reducing the size of the active space down to three orbitals based on the natural orbital occupation number (NOON) and averaging the qubits, we are left with a three-

https://doi.org/10.1021/acs.jctc.4c00915
J. Chem. Theory Comput. XXXX, XXX, XXX−XXX

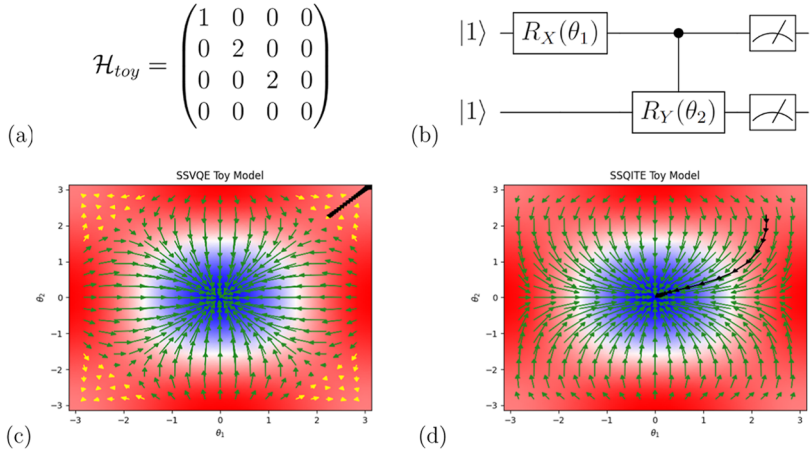

Figure 6. Comparison of SSVQE and SSQITE on a toy model with local minima. (a) The 2-qubit toy Hamiltonian with local minima. (b) The two-parameter ansatz used. (c, d) SSVQE and SSQITE applied to the three lowest states of this Toy Hamiltonian and ansatz pair. The orthogonal input states are $|11\rangle$, $|00\rangle$, and $|01\rangle$, respectively. The background coloring represents the weighted loss of the three lowest energy levels. SSVQE is unable to escape the local minima labeled with yellow arrows, while SSQITE is easily able to escape this minima. The black arrows represent a single run of SSVQE and SSQITE from the starting point $\theta_1 = \theta_2 = 2.3$, on the edge of the local minima.

qubit LiH Hamiltonian under the STO-6G basis.[42,43] We note that the model Hamiltonian studied here involves a representation of the LiH based on a truncated atomic orbital basis set that includes only s orbitals.[44] To match the experimental values for the LiH molecule, extended basis sets need to be incorporated into its Hartree−Fock calculations,[45,46] which is outside the scope of this paper.

Figure 5(a,c) shows the three lowest energy eigenvalues of LiH as a function of the interatomic Li−H distance for the noiseless [Figure 5(a)] and noisy [Figure 5(c)] SSQITE optimization. The results show excellent agreement with benchmark calculations for the entire range of interatomic distances.

Figure 5(b,d) shows the errors of SSQITE calculations for the LiH model, which remain within chemical accuracy. Similarly to the performance for the H_2 molecule, SSQITE performs well in calculations of ground and excited state energies of LiH. In fact, as shown in Figure 5, the noiseless (noisy) algorithm exhibits a maximum deviation of 1.30×10^{-3} Ha (1.32×10^{-3} Ha), below the benchmark of 1.6×10^{-3} Ha. The noisy results perform remarkably similarly to the noiseless results for both H_2 and LiH for two reasons. First, the circuits employed have limited gate depth and are therefore resistant to noise. Second, the added gate noise delays convergence of the algorithm, reducing the effect of the noise at the cost of a small number of extra iterations.

Lastly, the SSQITE algorithm was compared to SSVQE on a simple toy Hamiltonian in Figure 6. This comparison was done across the lowest three states in the toy two-qubit Hamiltonian, with ansatz shown in Figure 6b. Using this toy model, it is shown that SSVQE can become trapped in local minima, whereas SSQITE can escape to the global minimum. In Figure 6, SSVQE becomes trapped in the local minimum located at $\theta_1 = \theta_2 = \pm \pi$, while SSQITE instead finds the global minimum at $\theta_1 = \theta_2 = 0$. As VarQITE applied to ground states has previously been demonstrated to have a resistance to local minima as compared to VQE with a gradient descent optimizer,[13] this toy model demonstrates that this resistance holds even when VarQITE is extended to excited state algorithms such as SSQITE.

6. CONCLUSIONS

We have introduced the SSQITE method for the computation of excited states using quantum devices. This method combines key aspects of the SSVQE and VarQITE methodologies. We demonstrated the capabilities of SSQITE by calculating the low-lying excited states of H_2 and LiH molecules. The results showed robustness in avoiding local minima and excellent agreement with numerically exact calculations. We also demonstrated the resistance of SSQITE to local minima through a simple toy model. Additionally, SSQITE is not sensitive to degenerate states, unlike folded-spectrum VQE or folded-spectrum VarQITE, which calculate excited states by altering the Hamiltonian to $(\mathcal{H} - E)^2$,[28,44] where E is the energy of interest.

We have shown that using VarQITE as a foundation for excited state algorithms offers potential benefits relative to VQE, since some local minima typically found during VQE gradient descent are absent in VarQITE.[13] We have demonstrated that this advantage persists when applied to excited state algorithms. Additionally, we anticipate that the subspace-search methodology implemented in SSQITE could also be applied to exploit the advantages in other algorithms such as the Quantum Iterative Power Algorithm (QIPA). QIPA uses an oracle which double-exponentiates the Hamiltonian $\alpha(-\tau\mathcal{H}) = e^{e^{-\tau\mathcal{H}}}$ in order to amplify the global minimum of any input state. This has been shown to require fewer iterations than VarQITE for quantum optimization of ground states.[14] This suggests that the combination of subspace-search and imaginary time quantum evolution methodologies could outperform other currently available algorithms for the computations of excited states.

■ ASSOCIATED CONTENT

Data Availability Statement

The Python code for the SSQITE simulations is available at this link.

https://doi.org/10.1021/acs.jctc.4c00915
J. Chem. Theory Comput. XXXX, XXX, XXX−XXX

AUTHOR INFORMATION

Corresponding Author

Cameron Cianci − *Physics Department, University of Connecticut, Storrs, Connecticut 06269, United States; Mirion Technologies (Canberra) Inc., Meriden, Connecticut 06450, United States;* orcid.org/0000-0001-5617-0293; Email: cameron.cianci@uconn.edu

Authors

Lea F. Santos − *Physics Department, University of Connecticut, Storrs, Connecticut 06269, United States*

Victor S. Batista − *Department of Chemistry, Yale University, New Haven, Connecticut 06520-8107, United States; Yale Quantum Institute, Yale University, New Haven, Connecticut 06511, United States;* orcid.org/0000-0002-3262-1237

Complete contact information is available at: https://pubs.acs.org/10.1021/acs.jctc.4c00915

Notes

The authors declare no competing financial interest.

ACKNOWLEDGMENTS

The authors acknowledge support from the National Science Foundation Engines Development Award: Advancing Quantum Technologies (CT) under Award Number 2302908. V.S.B. also acknowledges partial support from the National Science Foundation Center for Quantum Dynamics on Modular Quantum Devices (CQD-MQD) under Award Number 2124511.

REFERENCES

(1) Olivucci, M.; Sinicropi, A. *Theoretical and Computational Chemistry*; Elsevier, 2005; Vol. *16*, pp 1−33.

(2) Josefsson, I.; Kunnus, K.; Schreck, S.; Föhlisch, A.; de Groot, F.; Wernet, P.; Odelius, M. Ab initio calculations of x-ray spectra: Atomic multiplet and molecular orbital effects in a multiconfigurational scf approach to the l-edge spectra of transition metal complexes. *J. Phys. Chem. Lett.* **2012**, *3*, 3565−3570.

(3) Bauer, B.; Bravyi, S.; Motta, M.; Chan, G. K.-L. Quantum algorithms for quantum chemistry and quantum materials science. *Chem. Rev.* **2020**, *120*, 12685−12717.

(4) Motta, M.; Rice, J. E. Emerging quantum computing algorithms for quantum chemistry. *WIRES Comput. Mol. Sci.* **2022**, *12*, No. e1580.

(5) Feynman, R. P. Simulating physics with computers. *Int. J. Theor. Phys.* **1982**, *21*, 467−488.

(6) Georgescu, I. M.; Ashhab, S.; Nori, F. Quantum simulation. *Rev. Mod. Phys.* **2014**, *86*, 153−185.

(7) Fox, M. A. Excited States in Photochemistry of Organic Molecules Edited by Martin Klessinger (University of Munster) and Josef Michl (University of Colorado). VCH: New York. 1995. xxiv + 537 pp. $89.95. ISBN 1−56081−588−4. *J. Am. Chem. Soc.* **1996**, *118*, 1815−1816.

(8) Daley, A. J.; Bloch, I.; Kokail, C.; Flannigan, S.; Pearson, N.; Troyer, M.; Zoller, P. Practical quantum advantage in quantum simulation. *Nature* **2022**, *607*, 667−676.

(9) Kim, Y.; Eddins, A.; Anand, S.; Wei, K. X.; van den Berg, E.; Rosenblatt, S.; Nayfeh, H.; Wu, Y.; Zaletel, M.; Temme, K.; Kandala, A. Evidence for the utility of quantum computing before fault tolerance. *Nature* **2023**, *618*, 500−505.

(10) Tilly, J.; Chen, H.; Cao, S.; Picozzi, D.; Setia, K.; Li, Y.; Grant, E.; Wossnig, L.; Rungger, I.; Booth, G. H.; Tennyson, J. The Variational Quantum Eigensolver: A review of methods and best practices. *Phys. Rep.* **2022**, *986*, 1−128.

(11) Lee, S.; Lee, J.; Zhai, H.; Tong, Y.; Dalzell, A. M.; Kumar, A.; Helms, P.; Gray, J.; Cui, Z.-H.; Liu, W.; Kastoryano, M.; Babbush, R.; Preskill, J.; Reichman, D. R.; Campbell, E. T.; Valeev, E. F.; Lin, L.; Chan, G. K.-L. Evaluating the evidence for exponential quantum advantage in ground-state quantum chemistry. *Nat. Commun.* **2023**, *14*, No. 1952.

(12) Peruzzo, A.; McClean, J.; Shadbolt, P.; Yung, M.-H.; Zhou, X.-Q.; Love, P. J.; Aspuru-Guzik, A.; O'Brien, J. L. A variational eigenvalue solver on a photonic quantum processor. *Nat. Commun.* **2014**, *5*, No. 4213, DOI: 10.1038/ncomms5213.

(13) McArdle, S.; Jones, T.; Endo, S.; Li, Y.; Benjamin, S. C.; Yuan, X. Variational ansatz-based quantum simulation of imaginary time evolution. *npj Quantum Inf.* **2019**, *5*, No. 75.

(14) Kyaw, T. H.; Soley, M. B.; Allen, B.; Bergold, P.; Sun, C.; Batista, V. S.; Aspuru-Guzik, A. Boosting quantum amplitude exponentially in variational quantum algorithms. *Quantum Sci. Technol.* **2024**, *9*, No. 01LT01.

(15) Benedetti, M.; Fiorentini, M.; Lubasch, M. Hardware-efficient variational quantum algorithms for time evolution. *Phys. Rev. Res.* **2021**, *3*, No. 033083.

(16) González, L.; Escudero, D.; Serrano-Andrés, L. Progress and Challenges in the Calculation of Electronic Excited States. *ChemPhysChem* **2012**, *13*, 28−51.

(17) Serrano-Andrés, L.; Merch'an, M. Quantum chemistry of the excited state: 2005 overview. *J. Mol. Struct.: THEOCHEM* **2005**, *729*, 99−108. Proceedings of the 30th International Congress of Theoretical Chemists of Latin Expression.

(18) Matsika, S.; Krylov, A. I. Introduction: Theoretical Modeling of Excited State Processes. *Chem. Rev.* **2018**, *118*, 6925−6926.

(19) Benavides-Riveros, C. L.; Wang, Y.; Warren, S.; Mazziotti, D. A. Quantum simulation of excited states from parallel contracted quantum eigensolvers. *New J. Phys.* **2024**, *26*, No. 033020.

(20) Smart, S. E.; Mazziotti, D. A. Accelerated Convergence of Contracted Quantum Eigensolvers through a Quasi-Second-Order, Locally Parameterized Optimization. *J. Chem. Theory Comput.* **2022**, *18*, 5286−5296. PMID: 36048172.

(21) Wang, Y.; Mazziotti, D. A. Electronic excited states from a variance-based contracted quantum eigensolver. *Phys. Rev. A* **2023**, *108*, No. 022814.

(22) Higgott, O.; Wang, D.; Brierley, S. Variational Quantum Computation of Excited States. *Quantum* **2019**, *3*, No. 156.

(23) Lischka, H.; Nachtigallová, D.; Aquino, A. J. A.; Szalay, P. G.; Plasser, F.; Machado, F. B. C.; Barbatti, M. Multireference Approaches for Excited States of Molecules. *Chem. Rev.* **2018**, *118*, 7293−7361.

(24) Reiher, M.; Wiebe, N.; Svore, K. M.; Wecker, D.; Troyer, M. Elucidating reaction mechanisms on quantum computers. *Proc. Natl. Acad. Sci. U.S.A.* **2017**, *114*, 7555−7560.

(25) Nakanishi, K. M.; Mitarai, K.; Fujii, K. Subspace-search variational quantum eigensolver for excited states. *Phys. Rev. Res.* **2019**, *1*, No. 033062, DOI: 10.1103/PhysRevResearch.1.033062.

(26) Gocho, S.; Nakamura, H.; Kanno, S.; Gao, Q.; Kobayashi, T.; Inagaki, T.; Hatanaka, M. Excited state calculations using variational quantum eigensolver with spin-restricted ansätze and automatically-adjusted constraints. *npj Comput. Mater.* **2023**, *9*, No. 13.

(27) Jones, T.; Endo, S.; McArdle, S.; Yuan, X.; Benjamin, S. C. Variational quantum algorithms for discovering Hamiltonian spectra. *Phys. Rev. A* **2019**, *99*, No. 062304, DOI: 10.1103/PhysRevA.99.062304.

(28) Tsuchimochi, T.; Ryo, Y.; Ten-no, S. L.; Sasasako, K. Improved Algorithms of Quantum Imaginary Time Evolution for Ground and Excited States of Molecular Systems. *J. Chem. Theory Comput.* **2023**, *19*, 503−513.

(29) Koch, M.; Schaudt, O.; Mogk, G.; Mrziglod, T.; Berg, H.; Beck, M. E. A Variational Ansatz for Taylorized Imaginary Time Evolution. *ACS Omega* **2023**, *8*, 22596−22602.

(30) Kosugi, T.; Nishiya, Y.; Nishi, H.; Matsushita, Y.-i. Imaginary-time evolution using forward and backward real-time evolution with a

single ancilla: First-quantized eigensolver algorithm for quantum chemistry. *Phys. Rev. Res.* **2022**, *4*, No. 033121.

(31) Motta, M.; Sun, C.; Tan, A. T. K.; O'Rourke, M. J.; Ye, E.; Minnich, A. J.; Brandão, F. G. S. L.; Chan, G. K.-L. Determining eigenstates and thermal states on a quantum computer using quantum imaginary time evolution. *Nat. Phys.* **2020**, *16*, 205−210.

(32) Motta, M.; Kirby, W.; Liepuoniute, I.; Sung, K. J.; Cohn, J.; Mezzacapo, A.; Klymko, K.; Nguyen, N.; Yoshioka, N.; Rice, J. E. Subspace methods for electronic structure simulations on quantum computers. *Electron. Struct.* **2023**, *6*, No. 013001, DOI: 10.1088/2516-1075/ad3592.

(33) Parrish, R. M.; Hohenstein, E. G.; McMahon, P. L.; Martínez, T. J. Quantum Computation of Electronic Transitions Using a Variational Quantum Eigensolver. *Phys. Rev. Lett.* **2019**, *122*, No. 230401, DOI: 10.1103/PhysRevLett.122.230401.

(34) Stair, N. H.; Huang, R.; Evangelista, F. A. A Multireference Quantum Krylov Algorithm for Strongly Correlated Electrons. *J. Chem. Theory Comput.* **2019**, *16* (4), 2236−2245, DOI: 10.1021/acs.jctc.9b01125.

(35) Colless, J. I.; Ramasesh, V. V.; Dahlen, D.; Blok, M. S.; Kimchi-Schwartz, M. E.; McClean, J. R.; Carter, J.; de Jong, W. A.; Siddiqi, I. Computation of Molecular Spectra on a Quantum Processor with an Error-Resilient Algorithm. *Phys. Rev. X* **2018**, *8*, No. 011021.

(36) Parrish, R. M.; McMahon, P. L. *Quantum Filter Diagonalization: Quantum Eigendecomposition without Full Quantum Phase Estimation*. 2019; https://arxiv.org/abs/1909.08925.

(37) Tkachenko, N. V.; Cincio, L.; Boldyrev, A. I.; Tretiak, S.; Dub, P. A.; Zhang, Y. *Quantum Davidson Algorithm for Excited States*. 2023; https://arxiv.org/abs/2204.10741.

(38) Cortes, C. L.; Gray, S. K. Quantum Krylov subspace algorithms for ground- and excited-state energy estimation. *Phys. Rev. A* **2022**, *105*, No. 022417.

(39) Barron, G. S.; Gard, B. T.; Altman, O. J.; Mayhall, N. J.; Barnes, E.; Economou, S. E. Preserving symmetries for variational quantum eigensolvers in the presence of noise. *Phys. Rev. Appl.* **2021**, *16*, No. 034003.

(40) Runge, C. Über die numerische Auflösung von Differentialgleichungen. *Math. Ann.* **1895**, *46*, 167−178.

(41) Benavides-Riveros, C. L.; Chen, L.; Schilling, C.; Mantilla, S.; Pittalis, S. Excitations of Quantum Many-Body Systems via Purified Ensembles: A Unitary-Coupled-Cluster-Based Approach. *Phys. Rev. Lett.* **2022**, *129*, No. 066401, DOI: 10.1103/PhysRevLett.129.066401.

(42) Zong, Z.; Huai, S.; Cai, T.; Jin, W.; Zhan, Z.; Zhang, Z.; Bu, K.; Sui, L.; Fei, Y.; Zheng, Y.; Zhang, S.; Wu, J.; Yin, Y. Determination of molecular energies via variational-based quantum imaginary time evolution in a superconducting qubit system. *Sci. China: Phys., Mech. Astron.* **2024**, *67*, No. 240311.

(43) Hempel, C.; Maier, C.; Romero, J.; McClean, J.; Monz, T.; Shen, H.; Jurcevic, P.; Lanyon, B. P.; Love, P.; Babbush, R.; Aspuru-Guzik, A.; Blatt, R.; Roos, C. F. Quantum Chemistry Calculations on a Trapped-Ion Quantum Simulator. *Phys. Rev. X* **2018**, *8*, No. 031022.

(44) Tazi, L. C.; Thom, A. J. W. Folded Spectrum VQE: A Quantum Computing Method for the Calculation of Molecular Excited States. *J. Chem. Theory Comput.* **2024**, *20*, 2491−2504.

(45) Kahalas, S. L.; Nesbet, R. Electronic structure of LiH and quadrupole moment of Li7. *J. Chem. Phys.* **1963**, *39*, 529−544.

(46) Tung, W.-C.; Pavanello, M.; Adamowicz, L. Very accurate potential energy curve of the LiH molecule. *J. Chem. Phys.* **2011**, *134*, No. 064117, DOI: 10.1063/1.3554211.